PREPARATION AND OPERATIONS OF THE MISSION PERFORMANCE CENTRE (MPC) FOR THE COPERNICUS SENTINEL-3 MISSION

Assessment of Visible and Short Wavelength Radiometric Calibration using Vicarious Calibration Methods

Ref.: S3MPC.RAL.TN.010
Issue: 1.1
Date: 17/09/2020
Contract: 4000111836/14/I-LG

Customer: ESA	Document Ref.: S3MPC.RAL.TN.010
Contract No.: 4000111836/14/I-LG	Date: 17/09/2020
	Issue: Issue 1.1

Project:	PREPARATION AND OPERATIONS OF THE MISSION PERFORMANCE CENTRE (MPC) FOR THE COPERNICUS SENTINEL-3 MISSION		
Title:	Assessment of Visible and Short Wavelength Radiometric Calibration using Vicarious Calibration Methods		
Author(s):	Dave Smith		
Approved by:	Dave Smith	Authorized by	
Distribution:			
Accepted by ESA			
Filename	S3MPC_VIS_SWIR_Vicarious_Calibration_Issue 1.1.docx		

ACRI-ST
260 route du Pin Montard
06904 Sophia-Antipolis, France
Tel: +33 (0)4 92 96 75 00 Fax: +33 (0)4 92 96 71 17
www.acri-st.fr

Change Log

Version	Date	Changes
0.1	10-Jan-2020	First draft
1.0	24-Jan-2020	Issued for QWG
1.1	17-Sep-2020	Page header for pages 8 onward corrected

List of Changes

Version	Section	Answers to RID	Changes

Table of contents

List of Figures

List of Tables

1 Scope of Document / Introduction

This document compares the results from assessments of the absolute radiometric calibration of the SLSTR VIS and SWIR channels that have been performed by different groups. The analyses presented in this document include:

- RAL Space for the MPC comparisons with AATSR and MODIS-A over desert sites(§2.1).
- CNES assessment using the SADE/MUSCLE vicarious calibration system(§2.2).
- Radiative Transfer Modelling of the Libya-4 desert site by Rayference (§2.3).
- University of Arizona comparisons against in-situ field measurements of the Railroad Valley Playa RadCalNet site (§2.4).

In this technical note we use the following convention to report the radiometric difference, *rel_diff*, between the SLSTR measured reflectances or radiances R_{SLSTR} and that of the reference R_{ref}.

$$\text{rel\_diff} = \frac{R_{SLSTR}}{R_{ref}} = \%\text{difference}/100 + 1.0 \qquad \textbf{Eq. 1}$$

When combining and comparing the results, we need to account for differences in the reference sensors used in the analysis. For example, previous analysis of AATSR we found as systematic offset compared to MERIS of approximately 1.03 for channels S1-S3 [1] So, for instance, where AATSR is used as the reference for S1-S3, we adjust the calibration to that for MERIS by applying the corresponding difference reported in the literature.

We can adjust the result using:

$$\text{rel\_diff'} = \frac{R_{SLSTR}}{R_{ref}} \frac{R_{ref}}{R_{ref\_new}} \qquad \textbf{Eq. 2}$$

For example, R_{ref} is AATSR and R_{ref_new} is MERIS. Using all measurements, we produce a radiometric calibration adjustment to be applied to the L1b data products. This is primarily based on the SLSTR-A analysis but can be applied to SLSTR-B since these can be considered as equivalent sensors.

For the reported uncertainties we attempt to combine the information provided using the Guide to expression of Uncertainties in Measurement (GUM) [2]. We note that the reported uncertainties are a range from standard deviations of the averages to a full combined uncertainty.

2 Input Analysis

2.1 Analysis by RAL (MPC)

The analysis method used by RAL for the comparison of SLSTR-A and B to a reference sensor is based on the approach developed for AATSR as described in Smith and Cox 2012 [1]. The analysis uses top-of-atmosphere reflectance extracted from SLSTR Level-1 products over quasi stable desert sites using the S3ETRAC tool developed by ACRI, CNES and RAL. The sites used by RAL are a subset of those used by CNES for their analysis. We have chosen AATSR and MODIS-A as the reference sensors for this analysis where we have pre-existing extractions from the desert sites which allows us to use existing analysis tools developed for the AATSR analysis. Before performing the comparisons, we need to account for known differences between sensor's geometry or spectral response. Effects include:

- Differences in site spectrum due to atmospheric effects such as ozone, water vapour, Rayleigh scattering, C02 and CH4
- Spectral differences in the site surface

For the intercomparison method developed by RAL we use look up tables derived from atmospheric modelling (MODTRAN) and spectral profiles of the sites derived from time series of MERIS and GOME-2 spectra.

An obvious effect is the time difference between the SLSTR measurements and those of AATSR and MODIS-A. Here we rely on the stability of the reference sensors and the assumed stability of the calibration sites. For the desert sites, the long-term stability is estimated at <1% over several years based on analysis from multiple sensors [3]. Where no direct comparison between sensors is possible, we use a parameterisation of the site BRF derived from a reference sensor (e.g. AATSR) at the corresponding wavelength of interest to provide a correction for view and solar geometry. The analysis method is illustrated in Figure 2-1.

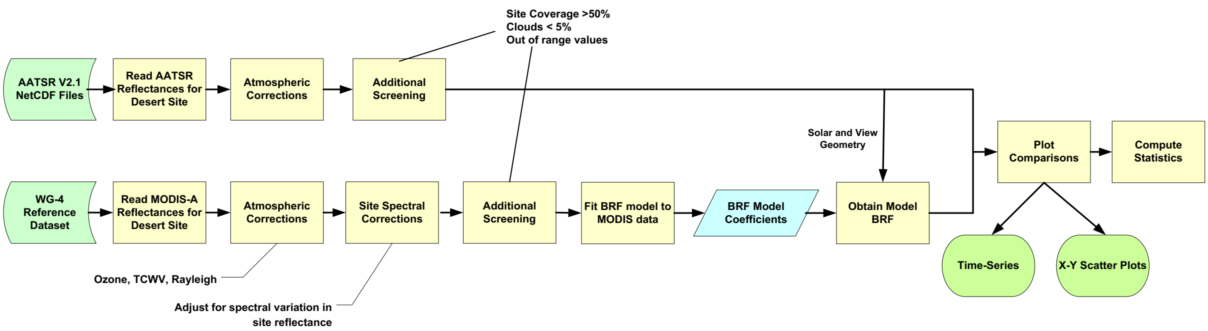

Figure 2-1: Example of indirect comparison between two sensors (in this case AATSR and MODIS AQUA)

After correcting for spectral differences, comparisons are performed by obtaining the BRF from the reference sensor where the corresponding view zenith, solar zenith and relative azimuth angles of SLSTR is found.

The relative differences and standard deviations, σ of the comparisons over all calibration sites processed are shown in Figure 2-2 and Figure 2-3. The average shown in Table 2-1 is weighted by the number of comparisons over each site, such that

$$\overline{\text{rel\_diff}} = \sum_{i=1}^{N} w_i \, \text{rel\_diff}_i \qquad \textbf{\textit{Eq. 3}}$$

and

$$w_i = n_i / \sum_{i=1}^{N} n_i \qquad \textbf{\textit{Eq. 4}}$$

where n_i is the number of observations over site *i*.

The combined standard deviation for the comparison is given by

$$\sigma^2 = \sum_{i=1}^{N} w_i \left(\text{rel\_diff}_i - \overline{\text{rel\_diff}}\right)^2 \Big/ (\text{N} - 1) + \sum_{i=1}^{N} (\, w_i \sigma_i)^2 \qquad \textbf{\textit{Eq. 5}}$$

We assume here that the standard deviations on the measurements are all uncorrelated.

For channels S3 and S5 there is good agreement of the results between all sites in nadir and oblique views. For S2 and particularly S1, there is more variability between sites. This could be due to the sensitivity of this channel to scattering as indicated by the larger standard deviations, but also the smaller number of match-ups – particularly in the oblique view. Results for Libya-4 have been shown separately for comparison with other methods presented in this report. However, the? results performed by RAL suggest that Libya-4 is fairly typical of the weighted average.

In Table 2-1 we include the results for the comparisons with MODIS Aqua over Libya-4. Here we notice that for S1-S3 there are noticeable differences in the results. These differences are most likely due to the relative differences between AATSR and MODIS-A as well as between AATSR and MERIS, Table 2-2 [from 1].

The adjusted differences to align to MERIS (for S1-S3) and MODIS (S5-S6) are given in Table 2-3.

For the uncertainties we have so far only considered the standard deviations results. Although these are a good indicator of the reproducibility they do not account for uncertainties in the adjustments or the modelling of the atmospheric corrections. For the adjustment factors we use the reported values in Table 2-2. For the modelling we have assigned a provisional 3% uncertainty for all spectral channels. Strictly speaking the uncertainty budget for the modelling should be broken down by band and contribution. E.g. S6 is sensitive to CH4, S3 to water vapour, S1 to aerosols.

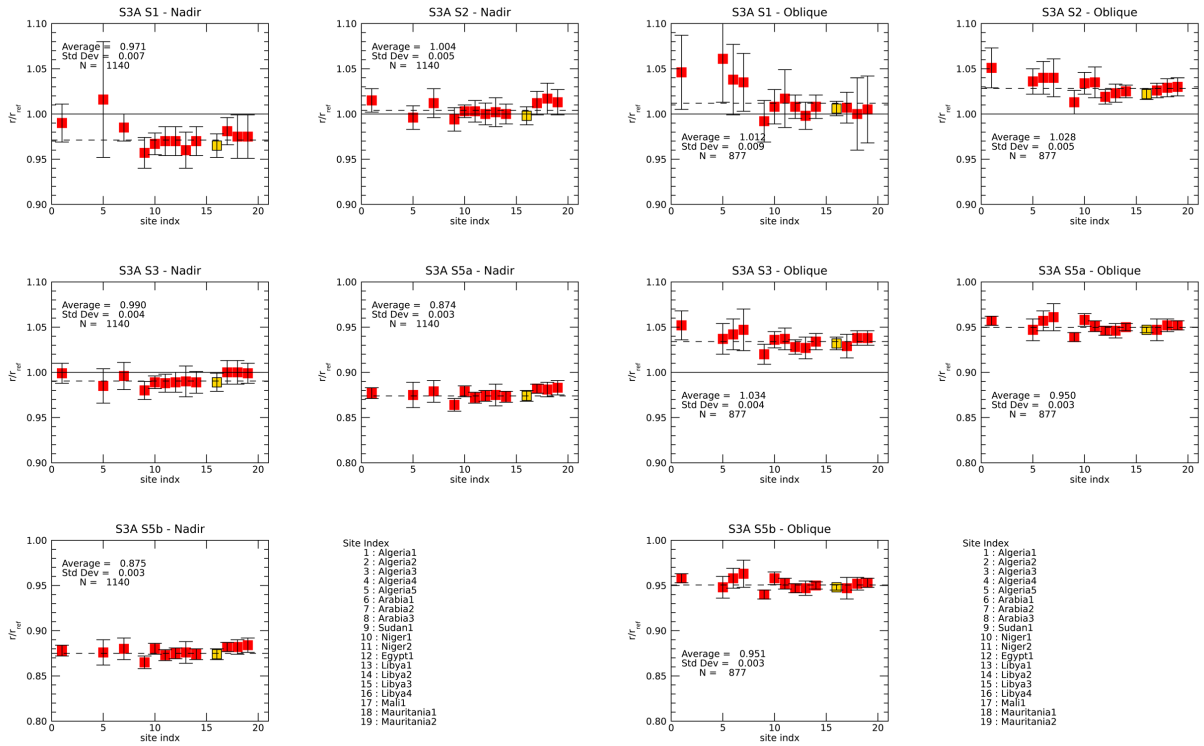

Figure 2-2: Results of comparisons between SLSTR-A nadir and oblique views and AATSR top-of-atmosphere reflectances for each desert site. The results presented in the box are the weighted averages of all the sites, the standard-deviation and the number of measurements used in the average. The results for Libya-4 are highlighted in yellow.

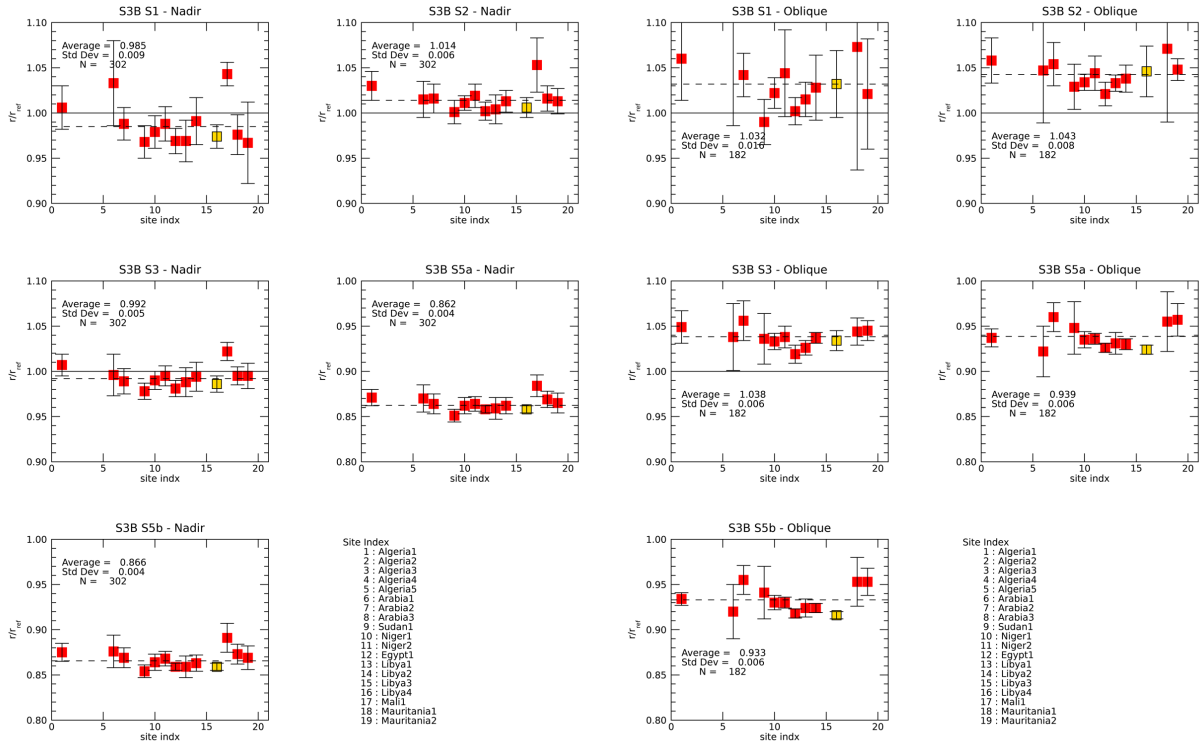

Figure 2-3: Results of comparisons between SLSTR-B nadir and oblique views and AATSR top-of-atmosphere reflectances for each desert site. The results presented in the box are the weighted averages of all the sites, the standard-deviation and the number of measurements used in the average. The results for Libya-4 are highlighted in yellow.

Table 2-1: Weighted mean value and standard deviation for SLSTR relative to AATSR and MODIS-A for the corresponding to the SLSTR spectral bands. MODIS-A data were from Libya-4 only.

SLSTR A

Nadir View

Method	S1		S2		S3		S5		S6	
	Rmeas/Rref	StdDev	Rmeas/Rref	StdDev	Rmeas/Rref	StdDev	Rmeas/Rref	StdDev	Rmeas/Rref	StdDev
Libya4 AATSR	0.965	0.013	0.998	0.010	0.989	0.010	0.874	0.006	-	-
Desert (All sites) AATSR	0.971	0.007	1.004	0.005	0.990	0.004	0.874	0.003	-	-
Libya4 MODIS-A	-	-	1.019	0.009	1.026	0.010	0.904	0.006	0.874	0.009

Oblique View

Method	S1		S2		S3		S5		S6	
	Rmeas/Rref	StdDev	Rmeas/Rref	StdDev	Rmeas/Rref	StdDev	Rmeas/Rref	StdDev	Rmeas/Rref	StdDev
Libya4 AATSR	1.006	0.008	1.022	0.006	1.032	0.007	0.947	0.004		
Desert (All sites) AATSR	1.017	0.009	1.029	0.005	1.035	0.004	0.954	0.003	-	-

SLSTR B

Nadir View

Method	S1		S2		S3		S5		S6	
	Rmeas/Rref	StdDev	Rmeas/Rref	StdDev	Rmeas/Rref	StdDev	Rmeas/Rref	StdDev	Rmeas/Rref	StdDev
SLSTR-A (Tandem)	1.022	0.027	1.005	0.005	1.000	0.017	0.992	0.017	0.995	0.015
Libya4 AATSR	0.974	0.013	1.006	0.011	0.986	0.009	0.858	0.004		
Desert (All sites) AATSR	0.985	0.009	1.014	0.006	0.992	0.005	0.864	0.004		
Desert MODIS-A			1.025	0.010	1.025	0.008	0.891	0.006	0.880	0.013

Oblique View

Method	S1		S2		S3		S5		S6	
	Rmeas/Rref	StdDev	Rmeas/Rref	StdDev	Rmeas/Rref	StdDev	Rmeas/Rref	StdDev	Rmeas/Rref	StdDev
SLSTR-A (Tandem)	1.002	0.008	1.000	0.005	0.985	0.005	0.982	0.003	1.007	0.003
Libya4 AATSR	1.032	0.037	1.046	0.029	1.035	0.011	0.930	0.004		
Desert (All sites) AATSR	1.032	0.016	1.043	0.008	1.038	0.006	0.935	0.007	-	-

Table 2-2: Mean value and standard deviation for AATSR relative to MERIS and MODIS-A corresponding to the SLSTR spectral bands S1-S3 and S6. [1]. MODIS-A data were from Libya-4 only.

Method	S1		S2		S3		S5	
	Rmeas/Rref	StdDev	Rmeas/Rref	StdDev	Rmeas/Rref	StdDev	Rmeas/Rref	StdDev
MERIS	1.015	0.032	1.012	0.030	1.023	0.025	-	-
MODIS	-	-	1.034	0.013	1.031	0.011	1.002	0.009

Table 2-3: Adjusted differences and standard deviation between S3A-SLSTR data compared to reference sensor using RAL inter-comparison method against AATSR adjusted to MERIS (S1-S3) and MODIS using reported calibration differences.

SLSTR A

Nadir View

Method	S1		S2		S3		S5		S6	
	Rmeas /Rref	StdDev	Rmeas/ Rref	StdDev	Rmeas/ Rref	StdDev	Rmeas/ Rref	StdDev	Rmeas/ Rref	StdDev
Desert (All sites) AATSR	0.986	0.007	1.016	0.005	1.013	0.017	0.876	0.017		
Libya4 MODIS-A			1.019	0.009	1.026	0.010	0.904	0.006	0.875	0.009
Average	**0.986**		**1.018**		**1.020**		**0.890**		**0.875**	
StdDev	0.007		0.006		0.013		0.022		0.009	
uAdjust	0.032		0.030		0.023		0.025		-	
uModel	0.030		0.030		0.030		0.030		0.030	
Combined Uncert	**0.044**		**0.043**		**0.040**		**0.045**		**0.031**	

Oblique View

Method	S1		S2		S3		S5		S6	
	Rmea/ Rref	StdDev	Rmeas/ Rref	StdDev	Rmeas/ Rref	StdDev	Rmeas/ Rref	StdDev	Rmeas/ Rref	StdDev
Desert (All sites) AATSR	1.027	0.009	1.041	0.005	1.058	0.004	0.952	0.003	-	-
Average	**1.027**		**1.041**		**1.058**		**0.952**		**-**	
StdDev	0.009		0.005		0.004		0.003		-	
uAdjust	0.032		0.030		0.023		0.025		-	
uModel	0.030		0.030		0.030		0.030		-	
Combined Uncert	**0.045**		**0.043**		**0.038**		**0.039**		**-**	

Table 2-4: Adjusted differences and standard deviation between S3B-SLSTR data compared to reference sensor using RAL inter-comparison method against AATSR adjusted to MERIS (S1-S3) and MODIS using reported calibration differences.

SLSTR B

Nadir View

Method	S1		S2		S3		S5		S6	
	Rmea/ Rref	StdDev	Rmeas/ Rref	StdDev	Rmeas/ Rref	StdDev	Rmeas/ Rref	StdDev	Rmeas/ Rref	StdDev
Desert (All sites) AATSR	1.000	0.009	1.026	0.011	1.015	0.009	0.864	0.004		
Libya4 MODIS-A			1.025	0.009	1.025	0.008	0.891	0.006	0.880	0.012
Average	**1.000**		**1.026**		**1.020**		**0.878**		**0.875**	
StdDev	0.007		0.007		0.009		0.019		0.012	
uAdjust	0.032		0.030		0.023		0.025		-	
uModel	0.030		0.030		0.030		0.030		0.030	
Combined Uncert	**0.044**		**0.043**		**0.039**		**0.044**		**0.032**	

Oblique View

Method	S1		S2		S3		S5		S6	
	Rmeas/ Rref	StdDev	Rmeas/ Rref	StdDev	Rmeas/ Rref	StdDev	Rmeas/ Rref	StdDev	Rmeas/ Rref	StdDev
Desert (All sites) AATSR	1.027	0.016	1.041	0.008	1.058	0.006	0.952	0.007	-	-
Average	**1.027**		**1.041**		**1.058**		**0.952**		**-**	
StdDev	0.016		0.008		0.006		0.007		-	
uAdjust	0.032		0.03		0.023		0.025		-	
uModel	0.03		0.03		0.03		0.03		-	
Combined Uncert	**0.047**		**0.043**		**0.038**		**0.040**		**-**	

2.2 Analysis by CNES

CNES have performed an analysis of the SLSTR-A radiometric calibration using data from calibration sites processed through the SADE/MUSCLE system [4, 5]. The results presented in Table 2-5 are primarily over Pseudo-invariant calibration sites (PICS) used for temporal monitoring, as well as cross- calibration between sensors. The analysis uses a geometrical matching and a spectral interpolation (to account for differences in instrumental spectral responses) to compare the radiometry of two different sensors and check the consistency of their calibration. This can be done for all bands on the reflective domain (except for absorption bands). A known issue with channel S6 has been the correction for CH_4. The default value for 6S is 1.72ppm which was the value for early 1990s. This has since been rescaled to a concentration of 1.85ppm. Results for the Libya-4 site are included for comparison with the other methods used in this report. As with the comparisons performed by RAL, the Libya-4 site results are in agreement with the averages for all desert sites. The only exception is for S6 which appears to be lower than for the average of all sites.

Table 2-5: Mean relative difference and standard deviation between S3A-SLSTR data compared to reference sensor as reported by CNES inter-comparison methods [5]. Note that the comparisons are dependent on the reference sensor and any known offsets to a common reference sensor (i.e. MERIS) in the radiometric scaling have not been accounted for.

Nadir View

Method	S1		S2		S3		S5		S6	
	Rmeas/Rref	StdDev	Rmeas/Rref	StdDev	Rmeas/Rref	StdDev	Rmeas/Rref	StdDev	Rmeas/Rref	StdDev
Desert MODIS	1.050	0.033	1.028	0.030	1.030	0.025	0.892	0.017	0.894	0.029
Libya-4 MODIS	1.044	0.020	1.037	0.069	1.035	0.020	0.896	0.011	0.837	0.022
Desert MERIS	1.023	0.036	1.020	0.025	1.010	0.023	-	-	-	-
Libya-4 MERIS	1.021	0.018	1.021	0.015	1.012	0.014	-	-	-	-
Desert PARASOL	1.040	0.037	1.050	0.028	1.040	0.027	-	-	-	-
Libya-4 PARASOL	1.041	0.020	1.049	0.020	1.045	0.021	-	-	-	-
S2A	1.010	0.025	1.008	0.025	0.996	0.024	0.899	0.016	0.882	0.031
Libya-4 S2A	1.012	0.018	1.002	0.014	0.994	0.014	0.897	0.011	0.890	0.020
Desert L8	1.001	0.022	1.002	0.017	0.996	0.018	0.898	0.012	0.872	0.018
Libya-4 L8	1.003	0.015	1.002	0.013	0.995	0.013	0.899	0.009	0.872	0.017

Oblique View

Method	S1		S2		S3		S5		S6	
	Rmeas/Rref	StdDev	Rmeas/Rref	StdDev	Rmeas/Rref	StdDev	Rmeas/Rref	StdDev	Rmeas/Rref	StdDev
Desert MODIS	1.070	0.053	1.070	0.030	1.070	0.031	0.950	0.023	0.890	0.076
Desert PARASOL	1.040	0.037	1.050	0.028	1.040	0.027	-	-	-	-

As with the RAL analysis for AATSR, the differences between methods are dependent on the calibration of the reference sensor. In Lacherade et al [4] cross calibration results show relative differences between MODIS and PARASOL wrt. MERIS for the corresponding spectral bands as reproduced in Table 2-6

Table 2-6: Mean value and standard deviation for PARASOL and MODIS sensors relative to MERIS corresponding to the SLSTR spectral bands S1-S3 processed by pairs for the 400-900nm spectral range [4]. Number of input measurements for each sensor are provided and the number of matchups is reported for each reference sensor. In this analysis a total of 11,227 input measurements were processed for the time period from 01/05/2002 to 10/12/2009.

Method	S1		S2		S3	
	Rmeas/Rref	StdDev	Rmeas/Rref	StdDev	Rmeas/Rref	StdDev
MODIS	0.974	0.027	0.986	0.018	0.988	0.017
PARASOL	0.972	0.032	0.968	0.023	0.974	0.020

Table 2-7: Mean relative difference and standard deviation between S3A-SLSTR data compared to reference sensor using CNES intercomparison methods adjusted to MERIS as the common reference sensor using reported calibration differences.

Nadir View

Method	S1		S2		S3		S5		S6	
	Rmeas/Rref	StdDev	Rmeas/Rref	StdDev	Rmeas/Rref	StdDev	Rmeas/Rref	StdDev	Rmeas/Rref	StdDev
Desert MODIS	1.023	0.043	1.014	0.035	1.018	0.030	0.892	0.017	0.894	0.029
Desert MERIS	1.023	0.036	1.020	0.025	1.010	0.023	-	-	-	-
Desert PARASOL	1.011	0.049	1.016	0.036	1.013	0.034	-	-	-	-
Average	**1.019**	**0.043**	**1.017**	**0.033**	**1.014**	**0.030**	**0.892**	**0.017**	**0.894**	**0.029**

Oblique View

Method	S1		S2		S3		S5		S6	
	Rmeas/Rref	StdDev	Rmeas/Rref	StdDev	Rmeas/Rref	StdDev	Rmeas/Rref	StdDev	Rmeas/Rref	StdDev
Desert MODIS	1.042	0.059	1.055	0.035	1.057	0.035	0.950	0.023	0.890	0.076
Desert PARASOL	1.011	0.049	1.016	0.036	1.013	0.034	-	-	-	-
Average	**1.027**	**0.059**	**1.036**	**0.045**	**1.035**	**0.047**	**0.950**	**0.023**	**0.890**	**0.076**

2.3 Analysis by Rayference

Rayference have developed a radiometric model of the Libya-4 desert site to provide an absolute calibration reference. The Libya-4 Radiometric Calibration Reference (LRCR) simulates the TOA BRF using a model of the surface BRF and 4 different Radiative Transfer Models (RTMs) [6].

Table 2.1 presents a summary of the analysis performed by Rayference. For consistency with the rest of this document the results have been presented as the relative difference as defined in Eq. 1. For the combined result we have taken a simple unweighted average. The uncertainties reported by Rayference are the standard deviations of all the comparisons and does not consider systematic effects due to effects introduced by the RTM code or input parameters (atmosphere).

For the standard deviations of the averages in Table 2.1 we have assumed the individual measurements are all correlated since the input dataset is the same for each analysis and any statistical variations in the results are due to instrument effects (e.g. gain drift, noise) and variations at the site (wind speed).

For the combined uncertainty, we have included the estimated uncertainty of 2.1% for the LRCR methodology as reported in the uncertainty statement of the Rayference document.

Table 2-8: Mean relative difference and standard deviation between S3A/SLSTR data and Libya-4 Rayference Calibration Reference (LRCR) generated with 4 RTMs [6]

Nadir View

RTM	S1		S2		S3		S5		S6	
	Rmeas/Rref	StdDev	Rmeas/Rref	StdDev	Rmeas/Rref	StdDev	Rmeas/Rref	StdDev	Rmeas/Rref	StdDev
6SV	1.037	0.013	1.022	0.009	1.016	0.010	0.892	0.007	0.887	0.011
LibRadtran	1.054	0.014	1.031	0.009	1.024	0.011	0.898	0.007	0.900	0.010
RTMOM	1.055	0.015	1.039	0.011	1.024	0.011	0.916	0.008	0.908	0.012
ARTDECO	1.054	0.014	1.035	0.009	1.024	0.009	0.908	0.007	0.909	0.009
Average	**1.050**	**0.016**	**1.032**	**0.012**	**1.022**	**0.011**	**0.903**	**0.013**	**0.901**	**0.014**
Combined Uncertainty	**0.026**		**0.024**		**0.024**		**0.025**		**0.025**	

Oblique View

RTM	S1		S2		S3		S5		S6	
	Rmeas/Rref	StdDev	Rmeas/Rref	StdDev	Rmeas/Rref	StdDev	Rmeas/Rref	StdDev	Rmeas/Rref	StdDev
6SV	1.079	0.015	1.060	0.012	1.070	0.012	0.971	0.008	0.940	0.015
LibRadtran	1.094	0.018	1.072	0.013	1.074	0.013	0.978	0.008	0.961	0.013
RTMOM	1.097	0.017	1.080	0.012	1.077	0.012	1.003	0.007	0.971	0.011
ARTDECO	1.088	0.016	1.070	0.012	1.074	0.013	0.988	0.008	0.964	0.014
Average	**1.089**	**0.018**	**1.070**	**0.015**	**1.074**	**0.012**	**0.985**	**0.016**	**0.959**	**0.018**
Combined Uncertainty	**0.028**		**0.026**		**0.024**		**0.026**		**0.028**	

2.4 Analysis by University of Arizona

Jeff Czapla-Meyers from University of Arizona has been able to perform an analysis of Sentinel-3A data with data based on in-situ measurements of Railroad Valley Playa which is one of the RadCalNet sites [7]. Although there were 51 overpasses, the analyses are constrained to 6.5° view zenith angle and 2x2 pixel region of interest (~1km x 1km) resulting 11 match-ups[6]. Data for larger view angles were not included because the BRDF for the site does not currently extend beyond 6.5°. Uncertainties are 4% based on the RadCalNet uncertainty statement [8].

	S1		S2		S3		S5		S6	
	Rmeas/Rref	Uncert	Rmeas/Rref	Uncert	Rmeas/Rref	Uncert	Rmeas/Rref	Uncert	Rmeas/Rref	Uncert
Railroad Valley	1.020	0.040	1.020	0.040	1.020	0.040	0.920	0.040	0.880	0.040

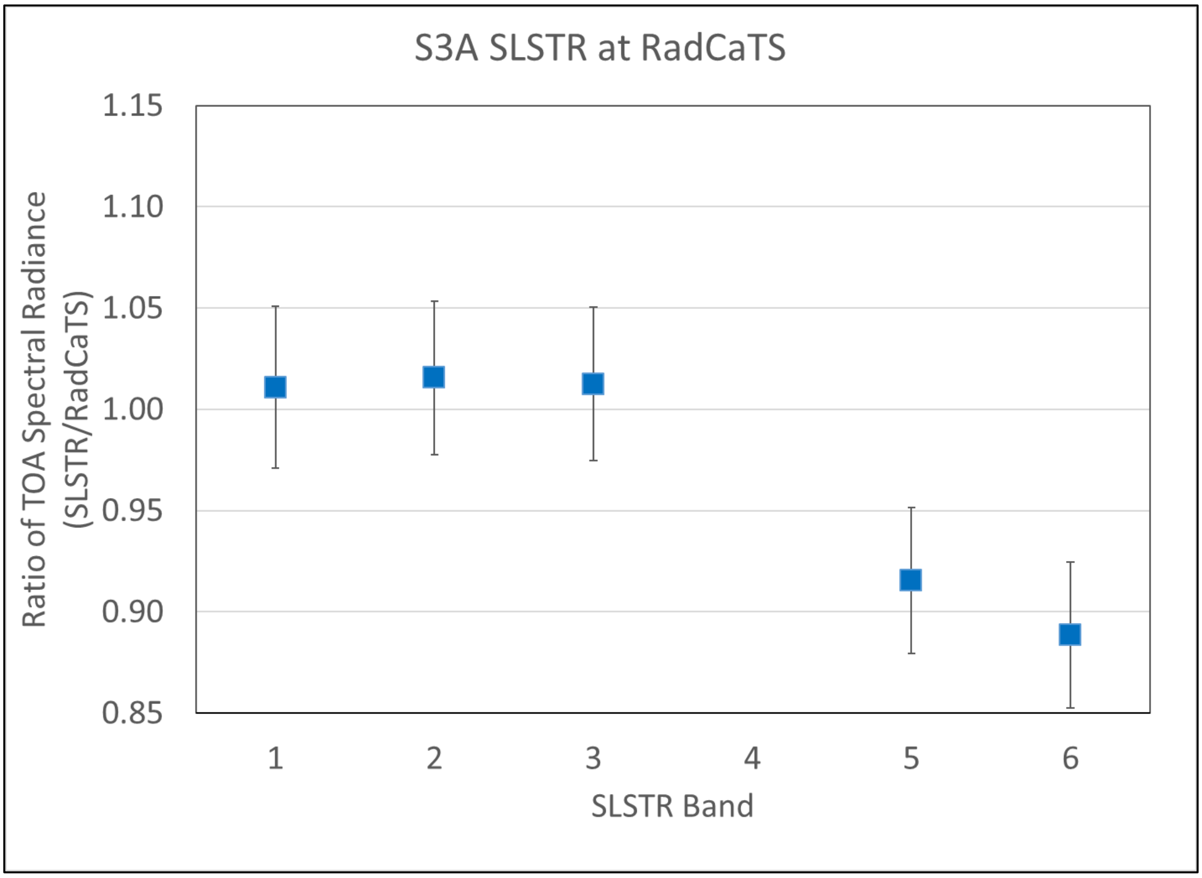

Figure 2-4: Results of comparisons of SLSTR TOA radiances compared with data derived from in-situ measurements at Railroad Valley Playa [7].

3 Combined Results

In Table 3-1 and Figure 3-1 we present the summary of all the analysis presented in this document. The values reported here have been rounded to 2 decimal places because uncertainty estimates are typically greater than 1%. RAL and CNES comparisons have been adjusted for known differences in the reference sensors show good agreement within the reported uncertainties.

For the combined result we present the median, unweighted and weighted averages. For the weighted averages we use Eq. 3 and weight according to the reported uncertainties so that greater weight is given to those measurements with lower uncertainty, such that

$$w_i = 1/\sigma_i \bigg/ \sum_{i=1}^{N} 1/\sigma_i \qquad \textbf{\textit{Eq. 6}}$$

We have assumed that uncertainties are uncorrelated. This is mainly because it is not possible to determine any degree of correlation between the methods. Although similar input data were used for the RAL, CNES and RTM analyses, the different approaches will each introduce additional effects that may or may not be correlated.

For the Nadir view, the median, unweighted and weighted averages are all equivalent. For the oblique view there is slightly more variability which is not surprising given that there are fewer observations contributing and the scatter in the input measurements larger.

Table 3-1: Summary of Vicarious Radiometric Calibration Results performed by all groups. Comparisons are performed by comparing the measured reflectance vs. reference reflectance. Results presented here are the ratios R_{meas}/R_{ref}.

Nadir View

Method	S1		S2		S3		S5		S6	
	Rmeas/Rref	Uncert	Rmeas/Rref	Uncert	Rmeas/Rref	Uncert	Rmeas/Rref	Uncert	Rmeas/Rref	Uncert
MPC (RAL)	-	-	1.02	0.04	1.02	0.04	0.89	0.04	0.88	0.03
CNES	1.02	0.05	1.02	0.05	1.01	0.04	0.89	0.03	0.89	0.04
RTM (Rayference)	1.05	0.03	1.03	0.03	1.02	0.03	0.90	0.03	0.90	0.03
RailRoad Valley	1.02	0.04	1.02	0.04	1.02	0.04	0.92	0.04	0.88	0.04
Median	**1.02**		**1.02**		**1.02**		**0.90**		**0.89**	
Average	**1.03**	**0.03**	**1.02**	**0.02**	**1.02**	**0.02**	**0.90**	**0.02**	**0.89**	**0.02**
Weighted Average	**1.03**	**0.03**	**1.02**	**0.02**	**1.02**	**0.02**	**0.90**	**0.02**	**0.89**	**0.02**

Oblique View

Method	S1		S2		S3		S5		S6	
	Rmeas/Rref	Uncert	Rmeas/Rref	Uncert	Rmeas/Rref	Uncert	Rmeas/Rref	Uncert	Rmeas/Rref	Uncert
MPC (RAL)	-	-	1.04	0.04	1.06	0.04	0.95	0.04	-	-
CNES	1.03	0.06	1.04	0.07	1.04	0.05	0.95	0.06	0.89	0.08
RTM (Rayference)	1.09	0.03	1.07	0.03	1.07	0.03	0.99	0.03	0.96	0.03
RailRoad Valley	-	-	-	-	-	-	--	-	-	-
Median	**1.09**		**1.04**		**1.06**		**0.95**		**0.96**	
Average	**1.06**	**0.06**	**1.05**	**0.04**	**1.06**	**0.03**	**0.96**	**0.03**	**0.92**	**0.07**
Weighted Average	**1.07**	**0.05**	**1.05**	**0.03**	**1.06**	**0.03**	**0.97**	**0.03**	**0.94**	**0.05**

Note: Uncertainty estimates are based on the reported uncertainties at k=1 and do not necessarily account for all effects.

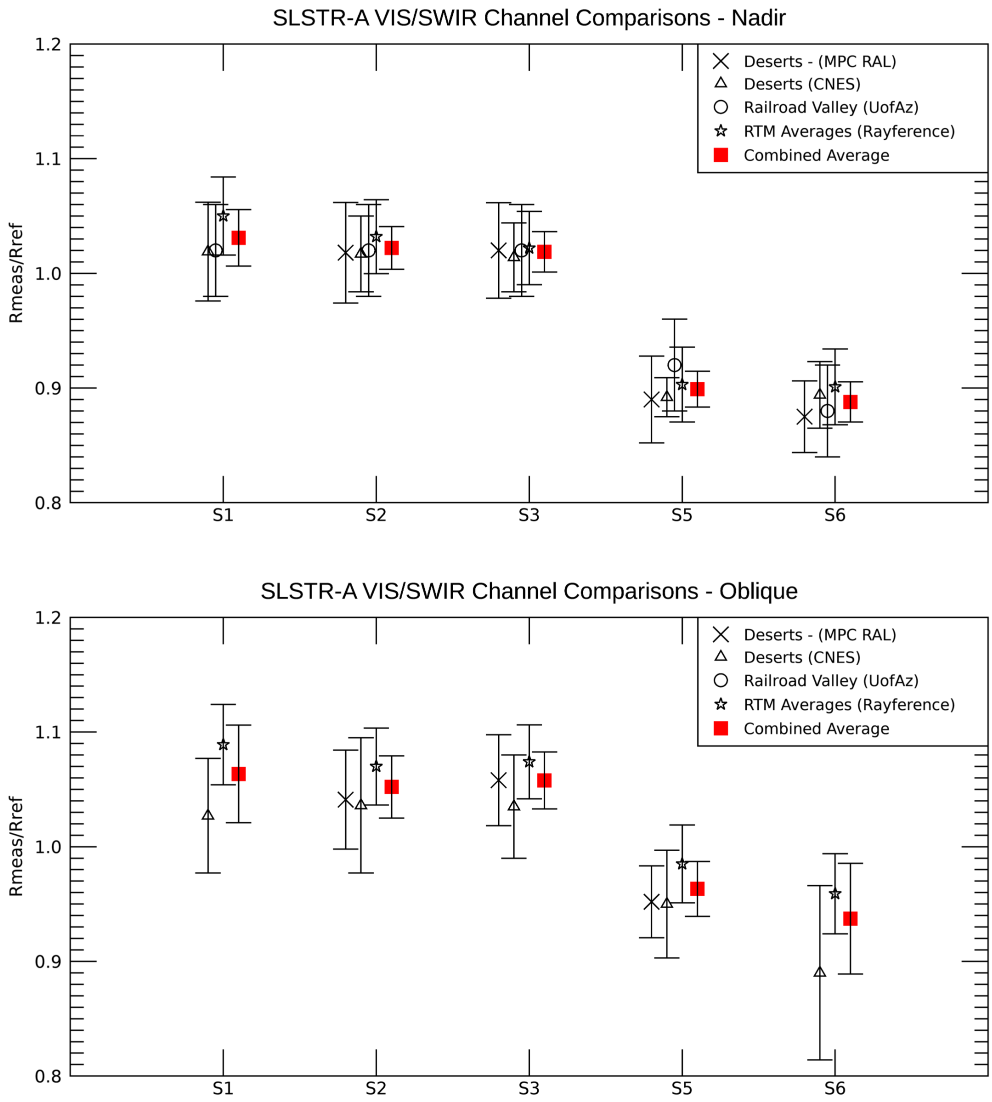

Figure 3-1: Summary of comparisons of SLSTR VIS/SWIR channel reflectances vs. Reference methods used to provide vicarious correction factors.

Table 3-2: Ratio Oblique to Nadir View relative differences.

Oblique wrt Nadir View

Method	S1		S2		S3		S5		S6	
	Rmeas/Rref	Uncert	Rmeas/Rref	Uncert	Rmeas/Rref	Uncert	Rmeas/Rref	Uncert	Rmeas/Rref	Uncert
Weighted Average	1.03	0.03	1.03	0.02	1.04	0.02	1.07	0.04	1.06	0.06

4 Correction factor to L1b products

The correction factor is the inverse of the vicarious calibration results – i.e. $1/(R_{meas}/R_{ref})$

The proposed vicarious adjustments have been based on analysis performed by the MPC by comparisons of SLSTR with MERIS via AATSR and MODIS-A over Desert Sites, CNES comparisons wrt. MODIS-A, measurements by University of Arizona over Railroad valley and radiative transfer modelling by Rayference.

Table 4-1: Proposed VIS-SWIR Calibration Adjustments Based on Vicarious Calibration analysis. Note S4 is not included because the vicarious calibration techniques do not extend to this band.

Nadir View

	S1	S2	S3	S5	S6
Correction	0.97	0.98	0.98	1.11	1.13
Uncertainty	0.03	0.02	0.02	0.02	0.02
Input Analysis	UoAz Rayference CNES	UoAz MPC (RAL) Rayference CNES	UoAz MPC (RAL) Rayference CNES	UoAz MPC (RAL) Rayference CNES	UoAz MPC (RAL) Rayference CNES

Oblique View

	S1	S2	S3	S5	S6
Correction	0.94	0.95	0.95	1.04	1.07
Uncertainty	0.05	0.03	0.03	0.03	0.05
Input Analysis	Rayference CNES	MPC (RAL) Rayference CNES	MPC (RAL) Rayference CNES	MPC (RAL) Rayference CNES	Rayference CNES

Note: Uncertainty estimates are at k=1.

5 Conclusions

We have compared the results of 4 different analysis of SLSTR top-of-atmosphere radiances over stable reference sites. The analyses show good agreement within the reported uncertainties. We do not attempt to state which method is closest to the true value since all methods are relative to a different reference.

Using the combined weighted averages, we are able to provide vicarious adjustment factors to align SLSTR reflectances to MERIS and MODIS Aqua L1 calibrations. This is on the basis that MERIS and MODIS calibrations have been assessed over many years and are considered as reference sensors in the VIS/SWIR [3]and relative differences with other sensors are reported [1, 4]. Alignment to a different reference sensor, e.g. Sentinel-2 would be possible provided that relative differences and uncertainty estimates are provided.

Uncertainties in the calibration factors are based on those reported by the different teams and are the best estimate at the time of writing.

We have not used results from other analyses methods such as comparisons over sun-glint scenes or Rayleigh scattering methods since these are relative inter-band methods and therefore sensitive to the radiometric calibration of the reference channel (e.g. S2 and S3 for Sun-Glint).

6 References

[1] Dave Smith and Caroline Cox, "(A)ATSR Solar Channel Calibration", IEEE Transactions on Geoscience and Remote Sensing, 51 (3), 1370-1382, 2013, 10.1109/TGRS.2012.2230333

[2] Joint Committee for Guides in Metrology: Evaluation of Measurement Data – Guide to the Expression of Uncertainty in Measurements 2008.

[3] Marc Bouvet, "Radiometric comparison of multispectral imagers over a pseudo-invariant calibration site using a reference radiometric model", Remote Sensing of Environment 140 (2014) 141–154, 10.1016/j.rse.2013.08.039

[4] Sophie Lacherade, Bertrand Fougnie, Patrice Henry and Phillipe Gamet, "Cross Calibration Over Desert Sites: Description, Methodology and Operational Implementation", IEEE Transactions on Geoscience and Remote Sensing, 51 (3), 1098-1113, 2013, 10.1109/TGRS.2012.2237061

[5] Desjardins…2019 e-mail

[6] Yves Goaverts, "Assessment of S3A/SLSTR Nadir and Oblique Solar Band Calibration over Libya-4", RAY-TN-201901, 2019

[7] Bouvet, M.; Thome, K.; Berthelot, B.; Bialek, A.; Czapla-Myers, J.; Fox, N.P.; Goryl, P.; Henry, P.; Ma, L.; Marcq, S.; Meygret, A.; Wenny, B.N.; Woolliams, "RadCalNet: A Radiometric Calibration Network for Earth Observing Imagers Operating in the Visible to Shortwave Infrared Spectral Range." E.R. *Remote Sens.* 2019, *11*, 2401., 10.3390/rs11202401

[8] Jeff Czapla-Meyers, E-Mail – 2019

[8] Jeff Czapla-Myers and Emma Woolliams "Uncertainty Analysis Statement – Railroad Valley USA", RadCalNet project document QA4EO-WGCV-IVO-CSP002, 2018

End of document